

# An Integrated Taguchi Design and Response Surface Methodological Approach for Development of Bedaquiline-Loaded Nanostructured Lipid Carriers

Rachmat MAULUDIN<sup>\*</sup>, Asti RAHAYU<sup>\*\*</sup>, SATRIALDI<sup>\*\*\*</sup>, Neng Fisher KURNIATI<sup>\*\*\*\*</sup>

*An Integrated Taguchi Design and Response Surface Methodological Approach for Development of Bedaquiline-Loaded Nanostructured Lipid Carriers*

## SUMMARY

Bedaquiline (BDQ), a poorly water-soluble drug, was successfully encapsulated in nanostructured lipid carriers (NLCs) to enhance its physicochemical properties. For the first time, BDQ-NLCs were optimized using a hybrid Taguchi and central composite design (CCD) methodology. This study selected cetyl palmitate, caprylic triglyceride, and Plantacare® 1200 in formulation development. The independent variables in this study, based on the Taguchi design approach, include the solid-liquid binary ratio, the surfactant concentration, and the sonication time. The dependent variables include particle size, encapsulation efficiency, and drug loading. The optimized BDQ-NLCs exhibited a particle size of  $153.5 \pm 2.3$  nm, an encapsulation efficiency of  $94.46 \pm 0.09\%$ , and a drug loading capacity of  $3.04 \pm 0.02\%$ . The characterization of the optimum BDQ-NLCs revealed a zeta potential of  $-47.75$  mV, a round particle morphology, and an endothermic event occurring between  $45.94$  and  $54.60^\circ\text{C}$ , indicating a transformation phase from solid to liquid. In vitro drug release profiles demonstrated that the optimized BDQ-NLCs formulation provides controlled and pH-dependent drug release, governed by a diffusion-driven mechanism. The stability evaluation of BDQ-NLCs demonstrated consistent stability under refrigerated conditions, while significant particle growth was observed at  $25^\circ\text{C}$  and  $40^\circ\text{C}$ , indicating temperature-dependent stability. Therefore, the developed BDQ-NLC formulation represents a physicochemically optimized system that may serve as a platform for further development of BDQ delivery, with therapeutic potential to be validated in future biological studies.

**Keywords:** Design of Experiment, Bedaquiline, characterization, formulation, nanostructured lipid carriers.

*Tasarım Deney Yöntemi Kullanılarak Nanoyapılı Lipid Taşıyıcılar, Tabletler ve İnsan Plazmasında Bedaquilin Fumarat Tayini İçin RP-HPLC Yönteminin Geliştirilmesi ve Validasyonu*

## ÖZ

Su içinde düşük çözünürlüğe sahip bir ilaç olan Bedaquiline (BDQ), fizikokimyasal özelliklerini iyileştirmek amacıyla nanoyapılı lipid taşıyıcılar (NLC'ler) içinde başarıyla enkapsüle edilmiştir. BDQ-NLC'lerin optimizasyonu, bir hibrit Taguchi ve merkezi kompozit tasarım (CCD) metodolojisi kullanılarak ilk kez bu çalışmada gerçekleştirilmiştir. Formülasyon geliştirmede setil palmitat, kaprilik trigliserit ve Plantacare® 1200 seçilmiştir. Taguchi tasarımına dayalı bağımsız değişkenler, katı-sıvı ikili karışım oranı, surfaktan konsantrasyonu ve sonikasyon süresini içermekte olup; bağımlı değişkenler ise parçacık boyutu, enkapsülasyon verimi ve ilaç yükü olarak belirlenmiştir. Merkezi Kompozit Tasarım ile geliştirilen optimize BDQ-NLC'ler,  $153,5 \pm 2,3$  nm'lik parçacık boyutu,  $94,46 \pm 0,09$  enkapsülasyon verimi ve  $3,04 \pm 0,02$  ilaç yük kapasitesi sergilemiştir. Optimum BDQ-NLC'lerin karakterizasyonu,  $-47,75$  mV'luk zeta potansiyeli, yuvarlak veya oval parçacık morfolojisi ve katı-sıvı faz dönüşümünü işaret eden  $45,94$  ile  $54,60^\circ\text{C}$  arasında gerçekleşen endotermik bir olay ortaya koymuştur. In vitro ilaç salım profilleri, optimize edilmiş BDQ-NLC'lerin difüzyon odaklı bir mekanizma ile kontrollü ve pH bağımlı bir ilaç salımı sağladığını göstermiştir. BDQ-NLC'lerin stabilite değerlendirmesi, soğutma koşullarında tutarlı bir kararlılık gösterirken,  $25^\circ\text{C}$  ve  $40^\circ\text{C}$ 'de anlamlı partikül büyümesinin gözlemlenmesi, sıcaklığa bağlı bir kararlılığı işaret etmektedir. Bu nedenle, geliştirilen BDQ-NLC formülasyonu, BDQ taşınmasının daha ileri geliştirilmesi için bir platform olarak hizmet edebilecek fizikokimyasal açıdan optimize edilmiş bir sistem olup, terapötik potansiyelinin gelecekteki biyolojik çalışmalarla doğrulanması gerekmektedir.

**Anahtar Kelimeler:** Deney Tasarımı, Bedaquilin, karakterizasyon, formülasyon, nanoyapılı lipid taşıyıcı.

Received: 11.11.2025

Revised: 19.02.2026

Accepted: 25.02.2026

<sup>\*</sup> ORCID: 0000-0002-3729-0254, Department of Pharmaceutics, School of Pharmacy, Institut Teknologi Bandung, Bandung, Indonesia

<sup>\*\*</sup> ORCID: 0009-0004-4731-942X, Program Doctoral, School of Pharmacy, Institut Teknologi Bandung, Bandung, Indonesia; Department of Pharmaceutics, Faculty of Health Sciences, Universitas PGRI Adi Buana Surabaya, Indonesia

<sup>\*\*\*</sup> ORCID: 0000-0001-9973-4044, Department of Pharmaceutics, School of Pharmacy, Institut Teknologi Bandung, Bandung, Indonesia

<sup>\*\*\*\*</sup> ORCID: 0000-0001-9973-4044, Department of Pharmacology and Clinical Pharmacy, School of Pharmacy, Institut Teknologi Bandung, Bandung, Indonesia

<sup>°</sup> Corresponding Author; Rachmat MAULUDIN  
E-mail: rachmat@itb.ac.id

## INTRODUCTION

*Mycobacterium tuberculosis* (MTB), the primary causative pathogen of tuberculosis (TB), remains a critical public health challenge worldwide (Millington et al., 2024). Following an upward trend in TB cases during the COVID-19 pandemic, the global incidence rate has shown a decline in growth and is now stabilizing (Bussi & Gutierrez, 2019). Reported cases reached around 10.8 million in 2023, marking a marginal increase from 10.7 million in 2022 but still substantially higher than the 10.4 million and 10.1 million recorded in 2021 and 2020, respectively. Additionally, in 2023, an estimated 175,923 patients globally were identified and received treatment for multidrug-resistant or rifampicin-resistant TB (MDR/RR-TB), accounting for only 44% of the projected 400,000 cases (with a 95% uncertainty interval ranging from 360,000 to 440,000) that emerged that year. Among recent advancements in TB treatment, BDQ stands out as an innovative oral diarylquinoline-based antimycobacterial drug (Luo et al., 2020). Approved by the FDA in 2012, BDQ has become a crucial therapeutic option for managing MDR and extensively drug-resistant TB (MDR/XDR-TB). Functioning as a first-in-class ATP synthase inhibitor, BDQ exhibits exceptional specificity toward mycobacteria (Wei et al., 2024), with a binding affinity for mycobacterial ATP synthase over 20,000 times stronger than for its eukaryotic counterpart (Abraham et al., 2024).

BDQ has been widely studied for alternative delivery methods, such as oral and intranasal administration (Chae, Choi, Tanaka, & Choi, 2021). Commercially available as *Sirturo*<sup>®</sup> by Janssen-Cilag, it is formulated as an uncoated 100 mg immediate-release tablet for oral ingestion (Guglielmetti et al., 2017). However, oral BDQ administration is often associated with adverse effects such as nausea, vomiting, joint pain, and QTc prolongation (Gavras & Schluger, 2024). To reduce these side effects, researchers have explored intranasal delivery systems that enable

direct lung targeting (Patil, Sawant, & Kunda, 2021). Despite this promise, achieving efficient pulmonary drug deposition, particularly in the alveolar region remains a significant challenge (Yadav, Rawal, & Baxi, 2016). Consequently, optimizing critical parameters like particle size, surface charge, and lipophilicity is essential to improve drug penetration across the respiratory barrier (Carnero Canales et al., 2024).

Currently, various methods are employed to address pulmonary barriers, including non-cellular and cellular barriers (Costabile et al., 2024). Among these, lipid-based nanoparticle carriers, or lipid nanocarriers, represent a promising approach (Gordillo-Galeano, Ospina-Giraldo, & Mora-Huertas, 2021). This methodology may enhance the pharmacodynamics of BDQ, addressing its poor aqueous solubility (0.002 µg/mL at 25°C) and high lipophilicity (log P ≈ 7.74) (PubChem). Nanostructured lipid carriers (NLCs) exhibit exceptional biocompatibility and drug-loading capacity, making them promising candidates for overcoming the solubility limitations of lipophilic drugs like BDQ (Jia et al., 2024). For example, research on the pulmonary administration of BDQ via nanolipid carriers for potential tuberculosis therapy highlights the critical role of targeted lung drug delivery in the effective management of respiratory diseases (De Matteis et al., 2018). NLCs constitute a superior generation of drug delivery vehicles, offering substantial improvements over conventional solid lipid nanoparticles. The strategic integration of liquid lipids into the NLC matrix fundamentally enhances system performance by overcoming multiple limitations of traditional formulations. These innovative carriers effectively resolve critical issues such as poor hydrophilic drug incorporation, reduced physical stability, and compound degradation, while simultaneously achieving superior drug payload capacity compared to earlier lipid-based systems (Mauludin, Garmana, & Fauzian, 2024; Müller, Radtke, & Wissing, 2002a). This unique structure not only enhances the payload capacity for lipophilic

drugs but also facilitates a sustained release profile, making NLCs a versatile platform for drug delivery (Kumar et al., 2023).

A significant gap exists in the current literature regarding the development of BDQ-NLCs using a hybrid Design of Experiments (DoE) methodology. This study bridges this gap by pioneering an integrated optimization strategy combining Taguchi design and CCD. The Taguchi method provides a robust screening phase, efficiently identifying critical formulation parameters with a minimal number of experimental runs through its orthogonal array design (Rajyalakshmi & Boggarapu, 2019). This synergistic Taguchi-CCD approach offers superior optimization capabilities compared to either method alone. The resulting optimized BDQ-NLCs formulation was thoroughly characterized for its particle size (PS), polydispersity index (PDI), zeta potential (ZP), entrapment efficiency (EE), drug loading (DL), and colloidal stability. Furthermore, we aimed to highlight the opportunity to integrate sustainable practices into the formulation development of our BDQ-NLCs by assessing our experimental designs and reducing energy and time consumption wherever possible.

## MATERIALS AND METHODS

### Materials

Bedaquiline fumarate with  $\geq 98.5$  % purity was procured from Hangzhou APIChem Technology Co., Ltd. Ammonium acetate was purchased from Merck KGaA, Darmstadt, Germany. Cetyl palmitate as Cutina<sup>®</sup> CP, Plantacare<sup>®</sup> 1200, Plantacare<sup>®</sup> 2000, Cremophor<sup>®</sup> RH 40, and Kolliphor<sup>®</sup> RH 40 were procured from BASF Co., Ltd. (Germany). Tego<sup>®</sup> Care 165 was procured from Evonik Co., Ltd (Germany). Capryl triglyceride, Span<sup>®</sup> 80, and Poloxamer 188 were obtained from Haihang Industry Co., Ltd. (China). The HPLC Grade Methanol and acetonitrile were acquired from Fisher Scientific Korea Ltd, Seoul, Korea. Analytical grade water (Onelab Waterone<sup>™</sup>) was obtained from PT. Jayamas Medica Industry (Sidoarjo, Indonesia).

## Methods

### Screening of lipids

The selection of solid and liquid lipids was based on their ability to solubilize BDQ. Solubility was assessed by incrementally adding solid lipids to 10 mg of BDQ at 80°C until no visible drug particles remained after 24 hours. Solubility behavior was evaluated visually via light microscopy. A lipid was deemed an effective solvent if it produced a clear solution (Satrialdi, Putri, & Lumintang, 2023); otherwise, it was classified as a non-solvent if a biphasic system formed (Kovačević, Müller, & Keck, 2020).

### The preparation of BDQ-NLCs

Surfactants were screened for their ability to emulsify solid-liquid binary mixtures. Initial NLCs were formulated by combining 5% (w/v) solid-liquid binary (SLB) ratio with 5% (w/v) surfactants or blends at 70°C, followed by 5-minute ultrasonication (CY-500, Optic Ivymen System<sup>®</sup>, Spain) at 60% amplitude. Emulsification efficiency was evaluated via particle size and PDI using a Delsa<sup>™</sup> Nano C Particle Analyzer (Beckman Coulter, USA).

### Experiment design for the optimization and development of BDQ-NLCs

A Taguchi design was used to screen critical formulation parameters for NLCs. Seven independent variables were investigated: SLB ratio ( $X_1$ ), total lipid amount ( $X_2$ ), surfactant concentration ( $X_3$ ), homogenization speed ( $X_4$ ), and homogenization time ( $X_5$ ), along with sonication amplitude ( $X_6$ ) and sonication time ( $X_7$ ), each evaluated at two concentration levels. This systematic approach assessed their influence on two critical quality attributes: particle size ( $Y_1$ ) and PDI ( $Y_2$ ). Statistical evaluation using Minitab software identified the most influential parameters through variance analysis, establishing their relative significance in the NLC fabrication process.

### Central composite design for formulation optimization

Building on the Taguchi design outcomes, three critical parameters—SLB ratio ( $X_1$ ), surfactant concentration ( $X_2$ ), and sonication time ( $X_3$ )—were further investigated using a CCD. The CCD was selected for its superior flexibility and accurate detection of non-linear relationships compared to other designs like Box-Behnken. This design evaluated the influence of these parameters on nanoparticle characteristics: particle size ( $Y_1$ ), encapsulation efficiency ( $Y_2$ ), and drug

$$Y_i = \beta_0 + \beta_1 X_1 + \beta_2 X_2 + \beta_3 X_3 + \beta_{11} X_{12} + \beta_{22} X_{22} + \beta_{33} X_{33} + \beta_{12} X_1 X_2 + \beta_{13} X_1 X_3 + \beta_{23} X_2 X_3$$

(Equation 1)

### Particle size, polydispersity index, and zeta potential determination

Particle size distribution and PDI were assessed by dynamic light scattering (DLS) following 20-fold dilution with Onelab Waterone™. Zeta potential measurements were conducted via electrophoretic light scattering (ELS) using a Malvern Instruments (UK) instrument, with 200-fold diluted samples analyzed in specialized flat-surface cells to ensure accurate surface charge determination.

### Encapsulation efficiency and drug loading determination

The encapsulation efficiency (EE) and drug load-

$$EE(\%) = \frac{\text{Theoretical BDQ Concentration} - \text{Free BDQ Concentration}}{\text{Theoretical BDQ Concentration}} \times 100\%$$

(Equation 2)

$$DL(\%) = \frac{\text{Amount of entrapped BDQ}}{\text{Amount of lipid phase} + \text{Amount of entrapped BDQ}} \times 100\%$$

(Equation 3)

### Morphology analysis

The morphology of BDQ-NLCs was analyzed using TEM (JEOL JEM-1400, Japan) at 100 kV. A drop of the optimized BDQ-NLCs was placed on a 200 nm carbon-coated copper grid. Negative staining was performed using UranylLess EM Stain, with 15  $\mu$ L applied for 1 min before imaging.

loading capacity ( $Y_3$ ). A total of 20 BDQ-NLC formulations were composed (Table 3.). ANOVA facilitated the selection of the most appropriate model, and response surface methodology generated polynomial equations (Equation 1.) to locate optimal formulation conditions. Model significance was determined by ANOVA ( $p < 0.05$ ), and validity was confirmed at a 95% confidence level by comparing predicted versus observed values. Subsequently, optimal conditions were established by applying specific criteria for each variable, ultimately identifying the solution with the highest desirability.

ing (DL) of BDQ-NLCs were determined through indirect quantification. Following centrifugation (13,000 rpm, 30 min) with a 10 kDa molecular weight cut-off filter (Amicon Ultra, USA), untrapped BDQ was extracted using methanol. Chromatographic separation was achieved using a LiChrospher C18 column with UV detection at 225 nm. The mobile phase consisted of ammonium acetate buffer (pH 4.7) and methanol (15:85 v/v), which was membrane-filtered (0.22  $\mu$ m) before use. Isocratic elution was maintained at 1.2 mL/min throughout the analysis. Results are reported as EE and DL, according to equations 1 and 2 below (Marques et al., 2025).

### Thermal characteristic determination

Thermal characterization was performed using a Shimadzu DSC-60 Plus calorimeter. Sample preparation involved centrifugation (10,000 rpm, 30 min) to minimize water interference. Precisely weighed samples (2-8 mg) of cetyl palmitate, unloaded NLCs, and optimized BDQ-NLCs were hermetically sealed

in aluminum crucibles. The temperature program ramped from 20°C to 90°C at 10°C/min, with a constant nitrogen purge at 50 mL/min. An empty aluminum pan provided the reference baseline for all measurements.

### In vitro drug release study

The *in vitro* release of BDQ-NLCs was evaluated using a dialysis bag method with a USP Apparatus II dissolution system. The study was conducted under sink conditions in two distinct media: phosphate buffer (pH 7.4) to simulate intestinal fluid and acetate buffer (pH 5.5) to mimic a moderately acidic environment. The dissolution vessel contained 900 mL of medium maintained at 37 ± 0.5°C with a paddle rotation speed of 100 rpm. An aliquot of BDQ-NLCs equivalent to 10 mg of BDQ was placed in a pre-hydrated dialysis bag (MWCO 12-14 kDa) and immersed in the release medium. Samples (5 mL) were withdrawn at predetermined intervals up to 2880 minutes, with immediate replenishment of fresh medium. BDQ concentration in the samples was quantified using a validated RP-HPLC method. Release kinetics were analyzed by fitting the cumulative release data to various mathematical models, with the best-fit model selected based on the highest coefficient of determination (R<sup>2</sup>). All experiments were performed in triplicate.

### Stability testing

The optimized BDQ-NLC formulation underwent stability testing under three temperature conditions (4°C, 25°C, and 40°C) for 30 days. Samples were analyzed at predetermined intervals (days 0, 7, 14, and 30) to evaluate particle size (PS), encapsulation efficiency (EE), and drug loading (DL) throughout the storage duration.

ciency (EE), and drug loading (DL) throughout the storage duration.

### Statistical analysis

Data analysis was performed using Minitab®21 software (Minitab, Inc., PA, USA). One-way analysis of variance (ANOVA) was used to determine intergroup differences, with p<0.05 set as the criterion for statistical significance. This threshold indicated significant differences between the experimental groups in the study.

## RESULTS AND DISCUSSION

### Classical lipid screening

The solubility profile of bedaquiline fumarate was systematically evaluated across eleven lipid excipients during a 60-minute observation period (Table 1.). Glyceryl monostearate (A1) demonstrated consistent solubility throughout all time points, whereas caprylic triglyceride (A7) required 30 minutes for complete dissolution. Partial solubility emerged after 45 minutes for cetyl palmitate (A2) and cetyl alcohol (A3), with remaining excipients showing no dissolution capacity. Comparative analysis identified glyceryl monostearate (A1) as the optimal excipient, followed by caprylic triglyceride (A7), with other lipids proving ineffective under experimental conditions (Pornputtapitak, Thiangjit, & Tantirungrotechai, 2024). Preliminary results suggest GMS may destabilize lipid nanoparticles, prompting the selection of cetyl palmitate for initial testing. Its composition—palmitic acid esterified with cetyl alcohol—provides a stable, adaptable matrix for drug encapsulation in NLCs (Kovačević et al., 2020).

**Table 1.** The solubility of Bedaquiline fumarate in various lipids

Time (min)	Lipid Excipients										
	A1	A2	A3	A4	A5	A6	A7	A8	A9	A10	A11
15	+	-	-	-	-	-	-	-	-	-	-
30	+	-	-	-	-	-	+	-	-	-	-
45	+	+	+	-	-	-	+	+	-	-	-
60	+	+	+	-	-	-	+	+	-	-	-

[(+) dissolved, (-) not dissolved]

### Selection of surfactants

Surfactant screening evaluated emulsification capacities for the SLB ratio (Figure 1). Lower-molecular-weight surfactants, such as Alkyl Polyglucosides (APGs), showed promising results (Sułek, Ogorzałek, Wasilewski, & Klimaszewska, 2013) and yielded smaller, more stable particle sizes. Lower molecular weight surfactants, such as Plantacare® 1200 (320.4 g/mol) and Plantacare® 2000 (345.8 g/mol), produced NLCs with smaller particle sizes ( $159.4 \pm 2.65$  nm and  $190.0 \pm 2.23$  nm) and lower PDI ( $0.190 \pm 0.003$  and  $0.206 \pm 0.005$ ), indicating superior uniformity and stability. In contrast, higher molecular

weight surfactants, such as Tego® Care 165 (~4,684.5 g/mol) and Pluracare® F 68 (~8,350 g/mol), resulted in larger particle sizes ( $839.5 \pm 1.35$  nm and  $747.2 \pm 2.54$  nm) and higher PDI ( $0.377 \pm 0.003$  and  $0.331 \pm 0.006$ ), suggesting reduced stability. Plantacare® 1200's shorter alkyl chain improved packing efficiency and reduced steric hindrance, yielding smaller particles. (Keck et al., 2014). High molecular weight surfactants, such as Tween® 80, Cremophor® RH 40, Kolliphor® RH 40, Tego® Care 165, and Poloxamer 188, often lead to destabilisation in NLC systems due to their increased steric hindrance and decreased diffusion rates at the oil-water interface.

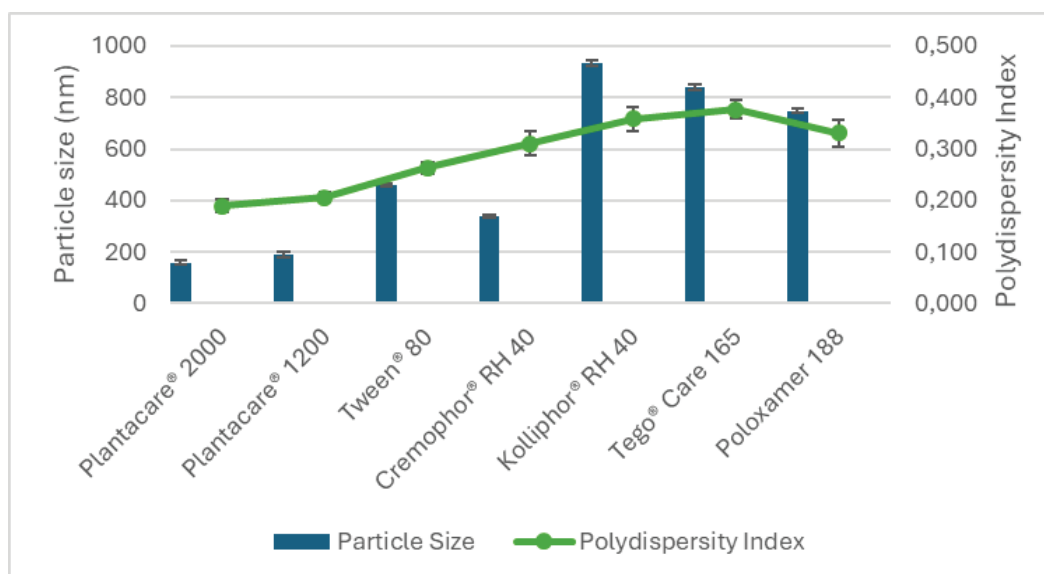


**Figure 1.** Particle size and PDI of the preliminary NLCs prepared from various surfactants, Plantacare® 2000; Plantacare® 1200; Tween® 80; Cremophor® RH 40; Kolliphor® RH 40; Tego® Care 165; and Poloxamer 188.

### Formulation development and optimization using a hybrid design approach: Taguchi design for screening of relevant experimental factors

The Taguchi method enables systematic optimization of formulation parameters, enhancing product consistency and quality (Rajyalakshmi & Boggarapu, 2019). This experimental configuration employs a specialized array design that enables comprehensive analysis of multiple variables within limited trials, accounting for linear, quadratic,

or higher-order effects while excluding factor interactions (Sathish, Giri, Rathinasamy, & Kanan, 2024). Particle size analysis demonstrated significant factorial modeling ( $p=0.0008$ ), with derived equations maintaining 95% confidence intervals, confirming robust statistical validity. The Taguchi design optimized BDQ-NLCs by focusing on particle size ( $Y_1$ ) and PDI ( $Y_2$ ) as critical quality attributes (Table 2.). Seven factors ( $X_1$ - $X_7$ ) at two levels each were tested across 16 formulations. Sonication amplitude ( $X_6$ ) had the greatest impact (rank 1), followed by

total lipid concentration ( $X_2$ , rank 2) and sonication time ( $X_7$ , rank 3). SLB ratio ( $X_1$ ) and homogenization speed ( $X_4$ ) were equally influential (rank 4), while homogenization time ( $X_5$ ) had the least effect (rank 7). The results highlight the importance of sonication parameters and lipid concentration in achieving

optimal particle size and uniformity. Although sonication amplitude ( $X_6$ ) and total lipid amount ( $X_2$ ) ranked highest for particle size control, the SLB ratio ( $X_1$ ) and surfactant concentration ( $X_3$ ) were prioritized for CCD optimization due to their critical influence on encapsulation efficiency and drug loading.

**Table 2.** Experimental design and results of BDQ-NLC formulations using the Taguchi method

Run	Experimental Factors							Dependent Variables	
Formulation	$X_1$	$X_2$	$X_3$	$X_4$	$X_5$	$X_6$	$X_7$	$Y_1$	$Y_2$
T1	60	4	3	6000	1	50	4	315	0.351
T2	60	4	3	8000	1	70	6	221	0.287
T3	60	4	5	6000	3	50	6	185	0.207
T4	60	4	5	8000	3	70	4	199	0.216
T5	60	6	3	6000	3	70	4	237	0.387
T6	60	6	3	8000	3	50	6	211	0.209
T7	60	6	5	6000	1	70	6	196	0.188
T8	60	6	5	8000	1	50	4	267	0.321
T9	80	4	3	6000	3	70	6	261	0.253
T10	80	4	3	8000	3	50	4	344	0.384
T11	80	4	5	6000	1	70	4	254	0.236
T12	80	4	5	8000	1	50	6	288	0.277
T13	80	6	3	6000	1	50	6	303	0.311
T14	80	6	3	8000	1	70	4	453	0.367
T15	80	6	5	6000	3	50	4	265	0.312
T16	80	6	5	8000	3	70	6	248	0.255

**Formulation optimization using central composite design**

The CCD offers superior methodological flexibility compared to the Box-Behnken Design in response surface methodology investigations. By incorporating axial points, CCD facilitates more accurate identification of nonlinear relationships between variables. This advanced design provides enhanced curvature detection and superior modeling capacity of response surfaces. Analysis of Taguchi results identified three key parameters: solid-liquid binary mixture ( $X_1$ ), surfactant concentration ( $X_2$ ),

and sonication time ( $X_3$ ) as the most influential experimental factors. The effects of these parameters on particle size ( $Y_1$ ), entrapment efficiency ( $Y_2$ ), and drug loading ( $Y_3$ ) were further investigated, and the CCD was employed to optimize the results. Outcomes from 20 experimental trials in this study are presented (Table 3.). Utilizing Central Composite Design, three polynomial equations were developed to assess variable-response correlations and determine optimal conditions. All models demonstrated strong predictive validity with regression coefficients ( $R^2$ ) > 0.800 (Table 4.), indicating excellent agreement between empirical data and theoretical predictions.

**Table 3.** Experimental design and results of BDQ-NLC formulations using the CCD

Run	Independent Variables			Dependent Variables			Polydispersity Index
	X <sub>1</sub>	X <sub>2</sub>	X <sub>3</sub>	Y <sub>1</sub>	Y <sub>2</sub>	Y <sub>3</sub>	
1	60	3.5	4	350	84.88	2.79	0.509
2	80	4.5	4	316	88.51	2.81	0.506
3	80	3.5	6	219	88.79	2.85	0.340
4	60	4.5	6	181	89.53	2.85	0.269
5	70	4	5	177	94.26	3.04	0.292
6	70	4	5	159	95.56	3.12	0.251
7	80	3.5	4	461	87.16	2.83	0.740
8	60	4.5	4	349	83.35	2.85	0.555
9	60	3.5	6	239	86.82	2.80	0.395
10	80	4.5	6	195	90.89	2.95	0.298
11	70	4	5	158	94.46	3.09	0.245
12	70	4	5	157	94.72	3.04	0.203
13	53.67	4	5	229	86.45	2.60	0.338
14	86.33	4	5	226	83.43	2.97	0.334
15	70	3.1835	5	215	86.34	2.89	0.337
16	70	4.8165	5	147	93.64	3.08	0.235
17	70	4	3.367	239	87.85	2.76	0.349
18	70	4	6.633	145	93.25	3.04	0.223
19	70	4	5	175	93.93	3.11	0.246
20	70	4	5	186	95.29	3.17	0.292

**Effect of experimental factors on particle size, entrapment efficiency, drug loading of BDQ-NLCs**

**Effect of experimental factors on particle size of BDQ-NLCs**

BDQ-NLCs particle size (147.5–461.7 nm) was significantly influenced ( $p < 0.05$ ) by sonication time ( $X_3$ ) and SLB ratio ( $X_2$ ). The coefficients of each variable facilitated a direct comparison of their effects on particle size, as indicated by the sign and magnitude of the coefficients. Regression analysis (Equation 4) revealed negative coefficients for both surfactant concentration (-25.4) and sonication duration (-59.7), demonstrating their inverse correlation with BDQ-NLC particle size. The larger magnitude of the sonication time coefficient indicates its greater relative impact on particle size reduction compared to surfactant concentration. Response surface methodology (Figure 4A.) confirmed that elevated levels of both parameters consistently

yielded smaller nanoparticles, with sonication time showing more pronounced effects on size diminution. Increased sonication time and surfactant concentration reduced particle size by forming a dense network, lowering interfacial tension, and preventing aggregation (Ma et al., 2014). The contour plots (Figure 4.) depict the response surfaces for PS, EE, and DL. In each plot, one independent variable was held at its hold values—surfactant concentration at 4% (w/v), sonication time at 5 min, and SLB ratio at 70, respectively. Prolonged ultrasonication enhances nanoparticle breakdown through cavitation-induced shear forces, effectively reducing particle size (Viegas et al., 2023). Conversely, elevated SLB ratio concentrations promote particle aggregation (Equation 4.), attributable to inadequate surfactant coverage, increased viscosity, and diminished sonication efficacy, ultimately yielding larger particle formations (Khosha, Reddi, & Saha, 2018).

Particle Size (nm):

$$166.9 + 5.0X_1 - 25.4X_2 - 59.7X_3 + 41.6X_1^2 + 24.2X_2^2 + 28.3X_3^2 - 13.7X_1X_2 - 10.3X_1X_3 + 9.0X_2X_3$$

(Equation 4)

### Effect of experimental factors on entrapment efficiency of BDQ-NLCs

Entrapment efficiency of BDQ-NLCs ranged from 83.35 to 95.56% (Table 3.). The ANOVA analysis revealed that the square effect of SLB ratio ( $X_1^2$ ), square effect of surfactant concentration ( $X_2^2$ ), square effect of sonication time ( $X_3^2$ ), variable surfactant concentration ( $X_2$ ), and sonication time ( $X_3$ ) significantly affect the entrapment efficiency of BDQ-NLCs (P-value < 0.05). While the effects of the variables  $X_2$  (surfactant concentration) and  $X_3$  (sonication time) were insignificant toward the BDQ-NLCs encapsulation efficiency (P-value > 0.05). Contour plot analysis (Figure 4B.) and (Equation 5.) show that elevated levels of the SLB ratio, surfactant concentration, and sonication time collectively enhance the encapsulation efficiency of BDQ-NLCs.

Increased surfactant concentration and prolonged sonication time reduce nanoparticle size, thereby increasing the surface area-to-volume ratio. This expanded interfacial area facilitates greater drug incorporation. During thermal processing, this promotes the preferential partitioning of BDQ into the lipid phase, thereby enhancing encapsulation efficiency during the subsequent homogenization and cooling stages (Beloqui, Solinís, Rodríguez-Gascón, Almeida, & Prést, 2016). Increased surfactant concentration stabilizes lipid nanoparticles, improving entrapment efficiency by minimizing aggregation (Khan, Sharma, & Jain, 2023). Prolonged sonication reduces particle size, strengthening drug-lipid interactions. Thermal processing dissolves BDQ, while subsequent cooling induces lipid solidification and drug entrapment. Size reduction through sonication enhances encapsulation efficiency via increased surface area.

Entrapment efficiency (%):

$$94.71 + 0.44X_1 + 1.24X_2 + 1.57X_3 - 3.71X_1^2 - 1.82X_2^2 - 1.61X_3^2 + 0.29X_1X_2 - 0.52X_1X_3 + 0.6X_2X_3$$

(Equation 5)

### Effect of experimental factors on drug loading of BDQ-NLCs

Drug loading of BDQ-NLCs varied from 2.60 to 3.17% (Table 3). According to the ANOVA analysis, the variables  $X_1$ , ratio of solid liquid mixture, square effect of SLB ratio ( $X_1^2$ ), and square effect of sonication time ( $X_3^2$ ) significantly affect the BDQ-NLCs drug loading (P-value < 0.05). In contrast, the variable surfactant concentration and sonication time were not significant for the BDQ-NLCs drug loading (P-value > 0.05). BDQ is the lipid-soluble active ingredient; therefore, the BDQ-NLCs drug loading was directly proportional to its encapsulation efficiency. On the contour plot (Figure 4C.) and according to (Equation 6.), it is shown that increasing the ratio of the solid-liquid lipid mixture ( $X_1$ ), the surfactant concentration

( $X_2$ ), and the sonication time ( $X_3$ ) will increase the BDQ-NLCs drug loading. The 20 tested BDQ-NLC formulas exhibited high encapsulation efficiency (>90%) (Table 3.). Elevating the solid-to-liquid lipid ratio improves active ingredient incorporation by forming a more rigid, organized matrix that can accommodate greater lipophilic drug content while reducing leakage potential. Higher solid lipid content enhances loading stability, whereas increased surfactant levels promote superior emulsification and nanoparticle stabilization through improved interfacial activity. This dual optimization strategy effectively balances drug payload with system stability (Khosa et al., 2018). Sonication time critically influences BDQ incorporation into NLCs by facilitating drug migration from the aqueous to the lipid phase during

hot homogenization. This redistribution process, enhanced by subsequent cooling, promotes effective encapsulation within lipid matrices. As previously

Drug loading (%)

$$3.09 + 0.06X_1 + 0.04X_2 + 0.05X_3 - 0.12X_1^2 - 0.05X_2^2 - 0.08X_3^2 - 0.004X_1X_2 + 0.02X_1X_3 + 0.01X_2X_3$$

(Equation 6)

The contour plots (Figure 4.) and optimization graphs (Figure 2.) provide critical insights into the relationships between independent variables and responses. Figure 4A reveals a nonlinear inverse correlation between sonication time ( $X_3$ ) and particle size ( $Y_1$ ), where extended sonication (>5 min) combined with higher surfactant concentrations ( $X_2$  >4% w/v) yielded particles below 200 nm, attributable to enhanced cavitation and interfacial stabilization. Conversely, Figure 4B demonstrates that encapsulation efficiency ( $Y_2$ ) plateaued at intermediate SLB ratio ( $X_1 \approx 70:30$ ) and surfactant levels ( $X_2 \approx 4\%$  w/v), reflecting a balance between lipid matrix capacity and surfactant-mediated drug partitioning. The global optimum (desirability = 0.9642) lies at the intersection of minimized particle size, maximized EE (>95%), and elevated drug loading (>3%), achieved at  $X_1 = 71.5:28.5$ ,  $X_2 = 4.2\%$  w/v, and  $X_3 = 5.4$  min (Figure 2.). These findings confirm the predictive accuracy of the quadratic models and highlight the need for multi-factor optimization for BDQ-NLCs. The optimized BDQ-NLCs achieved high encapsulation (94.46%) but moderate drug loading (3.04%), equating to a lipid-to-drug ratio of ~33:1. Administering a 100 mg BDQ dose would require approximately 3.3 g of lipid, a payload that is substantial yet potentially feasible for pulmonary delivery with optimized formulation strategies, though dose volume and local tolerability must be carefully evaluated. While the present study focuses on the physicochemical optimization and in vitro characterization of BDQ-NLCs, it is important

discussed, prolonged sonication time optimizes this phase-transfer mechanism, thereby improving overall drug-loading efficiency.

to note that demonstrating suitability for pulmonary delivery would require subsequent aerodynamic characterization in future studies.

### Selection of optimum BDQ-NLC formulation

The ideal BDQ-NLC formulation was determined using Table 4 criteria, demonstrating minimal particle diameter, maximal encapsulation efficiency, and optimal drug payload. Minitab® 21's response optimizer tool enabled this selection by systematically evaluating critical quality attributes. The optimization graphs reveal that the optimal values for the independent variables  $X_1$ ,  $X_2$ , and  $X_3$  are 71.5:29.5 for the Solid-liquid binary mixture, 4.2% (w/v) for the surfactant concentration, and 5.4 minutes for the sonication duration. The final optimized formulation was selected based on its superior performance across all critical parameters: it demonstrated (1) the smallest particle size ( $Y_1$ ) 141.1 nm, (2) the highest entrapment efficiency ( $Y_2$ ) 95.38%, and (3) the maximum drug loading ( $Y_3$ ) 3.12%, among all tested formulations, meeting our predetermined optimization criteria. A composite desirability value of 0.9642 was achieved for the optimized formulation, confirming its high reliability, where a value of 1.0 indicates all response goals are met simultaneously. This is visually supported by the optimization plots (Figure 2.), where the vertical lines pinpoint the optimal parameters (e.g., SLB ratio at 71.5) and the horizontal lines show the corresponding predicted responses (e.g., particle size of ~141 nm), collectively defining the global optimum.

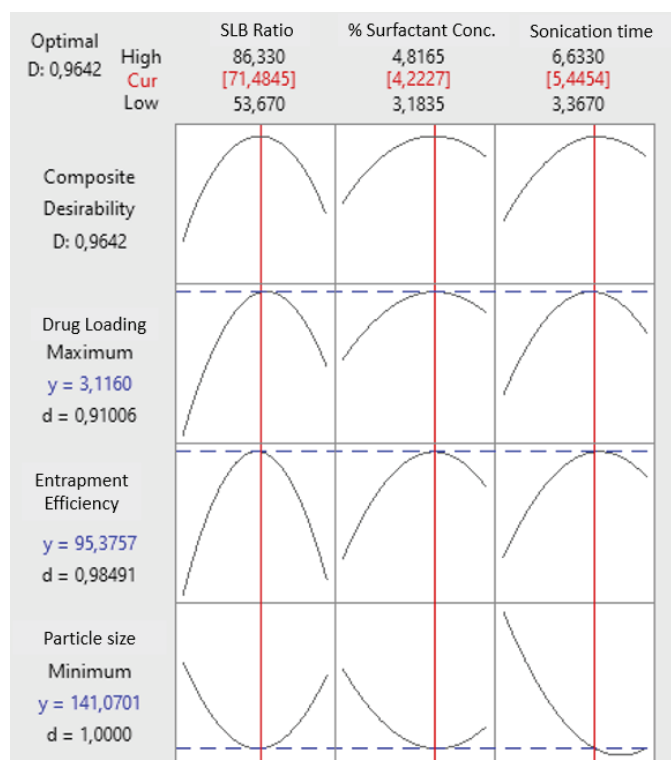


**Figure 2.** Optimization plots of  $Y_1$ : particle size (nm),  $Y_2$ : encapsulation efficiency (%), and  $Y_3$ : drug loading (%) based on independent variables  $X_1$ : SLB ratio (% w/v),  $X_2$ : surfactant concentration (% w/v), and  $X_3$ : sonication time (min).

### Confirmation of optimum BDQ-NLCs formulation

The BDQ-NLCs were fabricated utilizing the optimal formulation, and the outcomes were contrasted with the predicted values obtained from the CCD (Table 4.). The optimal formulation (Run 6) achieved a particle size of 159 nm, encapsulation efficiency of 95.56%, and drug loading of 3.12%, all of which closely matched the predictions with an error of less than 10%. This consistency underscores the robustness of the hybrid Taguchi-CCD approach in optimizing BDQ-NLCs. The experimental measurements for the responses  $Y_1$  (PS),  $Y_2$  (EE), and  $Y_3$  (DL) were found to be  $153.5 \pm 2.3$  nm,  $94.46 \pm 0.09\%$ , and  $3.04 \pm 0.02\%$ , respectively. The percentage of error calculated for the three responses was less than 10%, indicating that the predictive performance of models demonstrated significant predictive accuracy (Sabour & Amiri, 2017). Furthermore, the optimal BDQ-NLCs

formulation exhibited PDI and zeta potential values of  $0.29 \pm 0.03$  and  $-47.75 \pm 4.22$  mV, respectively. While the previous study achieved a smaller particle size of 65.57 nm, this can be attributed to their employment of high-shear homogenization (Rajendhiran & Bhattacharyya, 2024), a technique known to generate superior mechanical shear forces for nanoparticle size reduction compared to the ultrasonication method utilized in the present study. The optimized BDQ-NLCs showed higher entrapment efficiency attributed to the solid-liquid lipid ratio (71.5:29.5), Plantacare® 1200 surfactant (better stabilization), and extended sonication time (5.4 min) for improved drug encapsulation. This improvement likely results from our optimized solid-liquid lipid ratio (cetyl palmitate-caprylic triglyceride) and sonication parameters. The moderate drug loading (<5%) aligns with typical lipophilic drug limitations in NLCs due to lipid matrix crystallization. The value indicates a consistent particle

size distribution of the BDQ-NLCs, with no signs of particle aggregation. Meanwhile, the zeta potential value indicates excellent physical stability due to strong electrostatic repulsion between particles. This value is more negative than comparable Plantacare®

1200-based NLC systems, likely due to more uniform charge distribution from our optimized lipid-surfactant combination. The magnitude exceeding  $\pm 30$  mV (Müller, Radtke, & Wissing, 2002b) correlates with long-term colloidal stability.

**Table 4.** Comparison of the predicted and observed values from the optimized formulation

Response	Predicted value	Observed value	Error (%)
$Y_1$ : Particle size (nm)	141.1	153.5 $\pm$ 2.3	8.78
$Y_2$ : Entrapment efficiency (%)	95.38	94.46 $\pm$ 0.09	0.96
$Y_3$ : Drug loading (%)	3.12	3.04 $\pm$ 0.02	2.56

**Morphology analysis**

Transmission electron microscopy (TEM) analysis of the optimized BDQ-NLC formulation revealed well-defined spherical to oval nanoparticles (Figure 3.). The observed particle diameters (150-200 nm) correlated well with dynamic light scattering measurements,

confirming size uniformity. TEM micrographs showed discrete, non-aggregated particles with smooth surfaces, demonstrating excellent colloidal stability. This morphological characterization validates the successful preparation of monodisperse nanoparticles with the desired physicochemical characteristics.

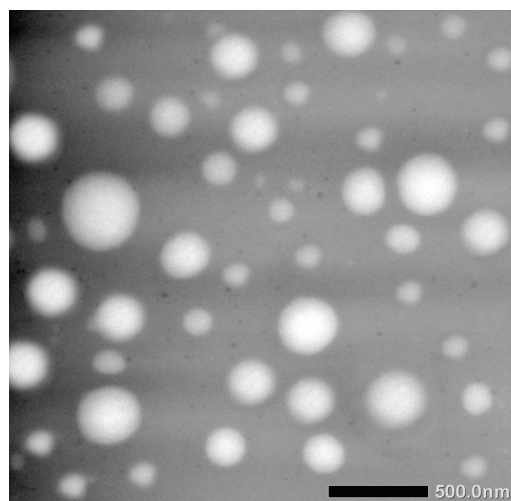


**Figure 3.** Transmission electron microscopy image showing the morphology of BDQ-NLCs at 25,000  $\times$  magnification.

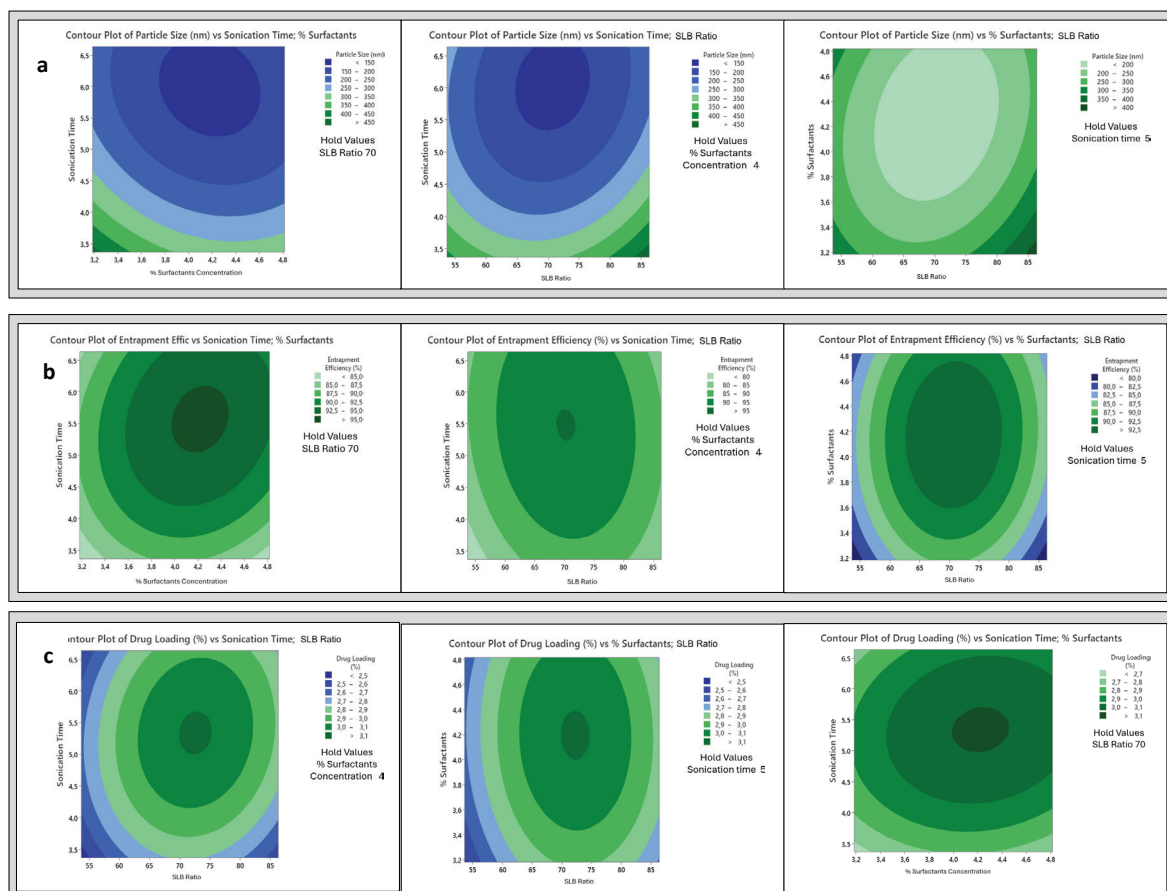


**Figure 4.** Contour plots for the effect of SLB ratio (% w/v), surfactant concentration (% w/v), and sonication time (min) on (a) particle size (nm); (b) encapsulation efficiency (%); (c) drug loading (%) of the BDQ-NLCs formula generated using CCD. In each plot, one independent variable was held at its hold values: surfactant concentration at 4% (w/v), sonication time at 5 min, and SLB ratio at 70, respectively.

### Thermal characteristic analysis

Differential scanning calorimetry (DSC) was employed to assess the thermal characteristics of NLCs and their individual components. Pure cetyl palmitate displayed a melting transition beginning at 47.74°C, reaching maximum heat flow at 56.37°C, and completing at 59.10°C, suggesting its broad phase transition range could affect lipid matrix stability. Unloaded NLCs demonstrated an endothermic peak centered at 51.03°C (range: 45.01–53.72°C), corresponding to the glass transition ( $T_g$ ) of the amorphous lipid phase, which represents a reversible thermodynamic process characteristic of disordered systems. The transition temperatures (onset, peak,

and endset) were lower in NLCs compared to pure cetyl palmitate. This depression results from the incorporation of caprylic triglyceride, which introduces structural disorder into the lipid matrix. BDQ-loaded NLCs exhibited modified thermal transitions with an onset at 45.94°C, peak at 51.93°C, and completion at 54.6°C, reflecting subtle drug-lipid interactions. Notably, the negligible difference ( $\Delta T = 0.9^\circ\text{C}$ ) in peak temperature between drug-loaded and blank NLCs indicates minimal perturbation of the lipid system by BDQ incorporation. The consistent appearance of endothermic transitions across all formulations verifies the preservation of a structurally intact solid lipid core in the NLC matrix (Müller et al., 2002b).

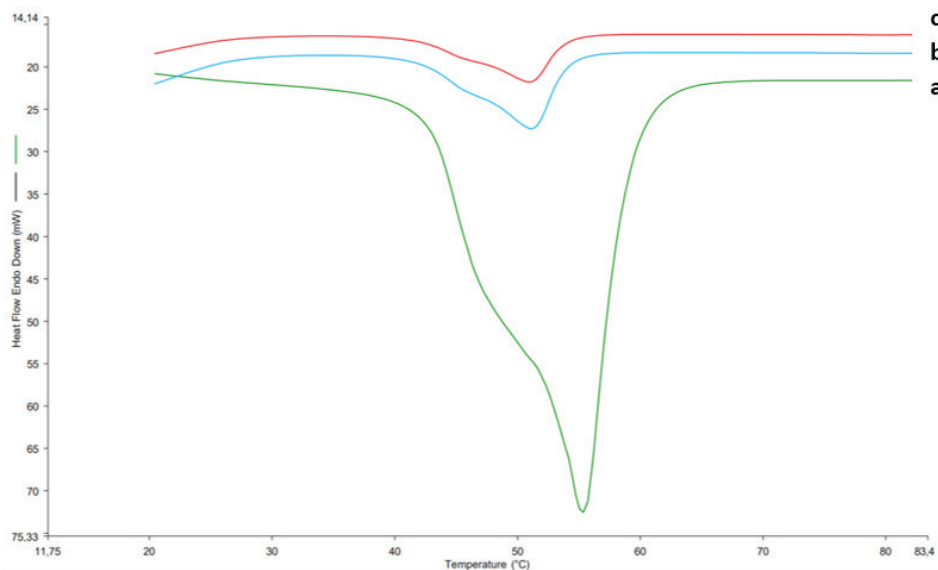


**Figure 5.** DSC thermograms of (a) cetyl palmitate; (b) blank NLCs; (c) BDQ-NLCs

***In vitro* drug release study**

The *in vitro* release study of BDQ-NLCs exhibited a pH-dependent release profile. At pH 7.4, the cumulative release was 65.78% over 2880 minutes, while a significantly higher release of 79.91% was achieved at pH 5.4 (Figure 6.). This enhanced release under acidic conditions suggests a favorable environment for BDQ diffusion from the lipid matrix. Kinetic modeling revealed that the release at both pH values best followed the Higuchi model ( $R^2 = 0.9747$  at pH 7.4;  $R^2 = 0.9706$

at pH 5.4), indicating a diffusion-controlled release mechanism (Table 5.). Furthermore, the Korsmeyer-Peppas model at pH 5.4 yielded a release exponent of 0.62, signifying a non-Fickian or anomalous transport where drug diffusion and lipid matrix erosion both contribute to the release kinetics. The sustained release profile across 2880 minutes demonstrates the potential of NLCs to provide prolonged BDQ delivery, which is advantageous for improving patient adherence in long-term tuberculosis therapy.

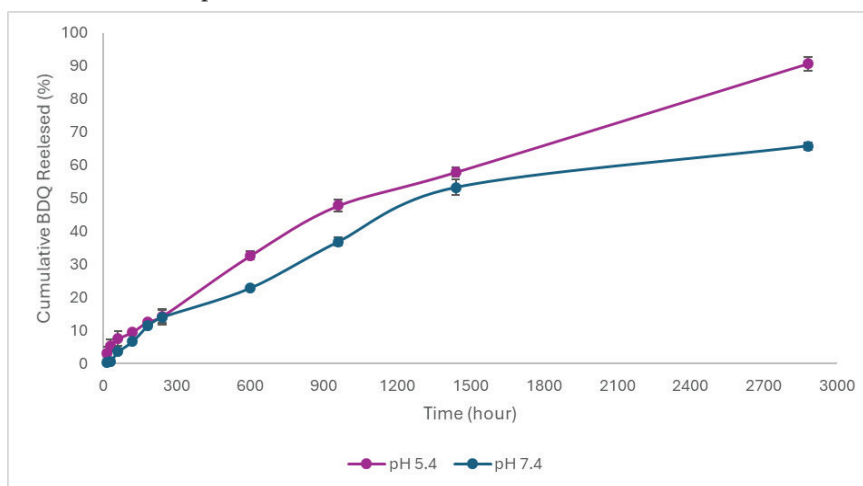


**Figure 6.** *In vitro* release profile of Bedaquiline (BDQ) from optimized nanostructured lipid carriers (NLCs) in two different pH media over 2880 minutes. The cumulative drug release (%) is plotted against time (minutes). Data are presented as mean  $\pm$  SD (n = 3).

**Table 5.** Kinetic model parameters for BDQ release from NLCs

pH	Zero-Order (R <sup>2</sup> )	First-Order (R <sup>2</sup> )	Higuchi (R <sup>2</sup> )	Korsmeyer-Peppas (R <sup>2</sup> )
7.4	0.9169	0.4924	0.9747	0.9843
5.4	0.9379	0.7264	0.9706	0.9802

**Stability study**

The stability assessment evaluates the optimal BDQ-NLCs formulation by examining parameters such as particle size, encapsulation efficiency, and drug loading over 30 days at storage temperatures of 4, 25, and 40°C, with findings presented in Figure 7. The optimal BDQ-NLC formulation demonstrated no significant increase in particle size (P-value > 0.05) at day 30 (172.5 ± 11.9 nm) compared to the initial measurement at day 0 (153.5 ± 2.3 nm) when stored at 4°C. Significant increases in particle size (P-value < 0.05) were observed at both 25°C and 40°C. The BDQ-NLCs stored at 25°C exhibited an increase in particle size starting on day 30 (164.8 ± 8.7 nm), while at 40°C, the increase was observed from day 28 (174.8 ± 7.2 nm) compared to the initial size. The

optimal BDQ-NLC formulation showed no significant changes in PDI or encapsulation efficiency (EE) over 30 days at 4°C, 25°C, and 40°C. PDI values remained below 0.5, indicating stable particle size distribution, while EE consistently ranged from 90-95%, confirming effective BDQ retention in the NLC matrix throughout storage. The significant increase in particle size at 25°C and 40°C suggests that the formulation is susceptible to aggregation under ambient and accelerated conditions. Therefore, refrigerated storage (4°C) is recommended to maintain colloidal stability during storage. Stability at 4°C is attributed to strong electrostatic forces and reduced kinetic energy, while elevated temperatures increase kinetic energy, promoting particle collisions and aggregation, leading to instability.

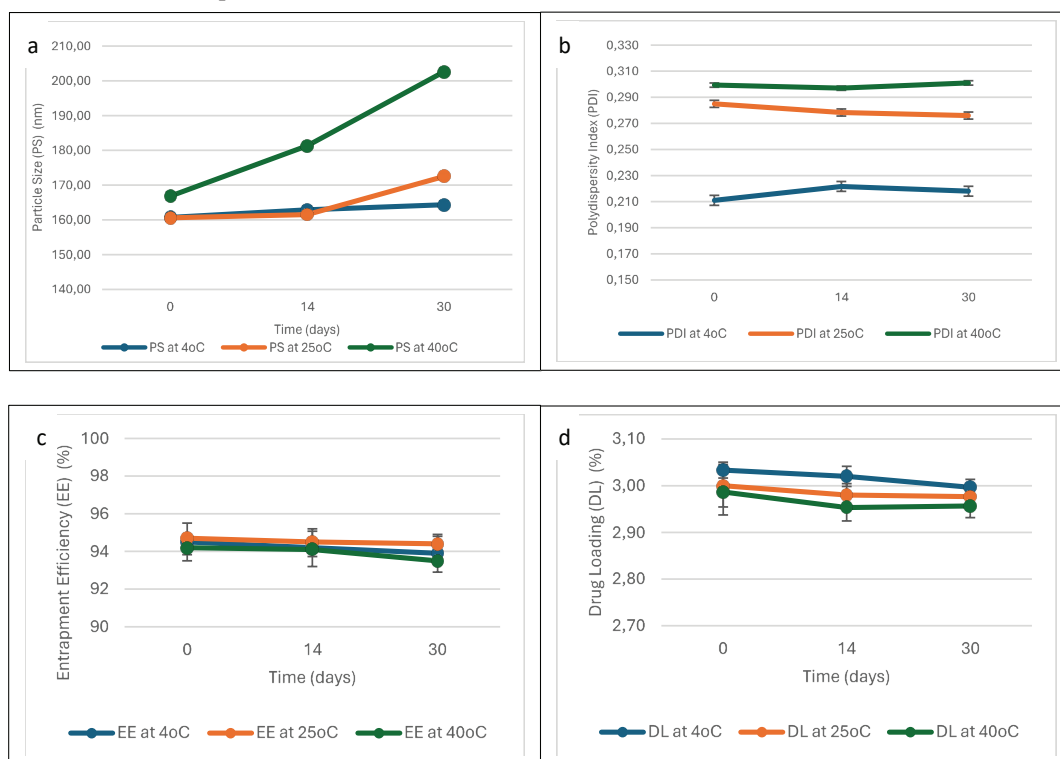


**Figure 7.** Stability assessment over a period of 30 days, focusing on (a) particle size; (b) PDI; (c) encapsulation efficiency; and (d) drug loading. The data, presented as mean ± standard deviation (n=3), demonstrate significant changes (\*P < 0.05) compared to the initial measurements.

## CONCLUSIONS

BDQ-NLCs were optimized using a Taguchi design followed by a central composite design, integrating DoE to identify critical factors and predict optimal conditions. Key factors influencing NLC quality included the solid-liquid binary mixture, surfactant concentration, and sonication time. BDQ was successfully incorporated into NLCs via hot homogenization-ultrasonication, enhancing its physicochemical properties. The optimized BDQ-NLC formulation consisted of a solid-to-liquid lipid ratio of 71.5:29.5, a surfactant concentration of 4.2% (w/v), and a sonication time of 5.4 minutes. This formulation yielded an optimal NLC system with a particle size of  $153.5 \pm 2.3$  nm, PDI of  $0.31 \pm 0.04$ , an encapsulation efficiency of  $94.46 \pm 0.09\%$ , and a drug loading capacity of  $3.04 \pm 0.02\%$ . Further characterization of the optimized BDQ-NLCs revealed a zeta potential of  $-47.75 \pm 3.21$  mV and a spherical or oval particle morphology, as confirmed by TEM analysis. DSC analysis indicated an endothermic event between  $45.94^\circ\text{C}$  and  $54.60^\circ\text{C}$ , with a peak at  $51.93^\circ\text{C}$ . The in vitro release profile demonstrated a sustained and pH-dependent controlled release, governed by a diffusion-driven mechanism. The stability assessment was conducted over 30 days under controlled conditions. Long-term stability studies under varied storage environments would be valuable to further establish the shelf-life of the formulation. Future work should include biological assays such as MIC determination and cytotoxicity evaluation to assess therapeutic potential.

## ACKNOWLEDGEMENTS

The authors gratefully acknowledge the financial support provided by the Overseas Research Grant from The Asahi Glass Foundation (Contract No: 1835/IT1.B07.1/TA.00/2025) for this research endeavor.

## AUTHOR CONTRIBUTION STATEMENT

Concept (AR, RM), Design (AR, RM), Supervision (RM, ST, NFK), Resources (AR, RM), Materials (AR, RM), Data Collection and/or Processing (RM, AR), Analysis and/ or Interpretation (RM, ST, NFK), Literature Search (RM, AR), Writing (RM, AR), Critical Reviews (RM, ST, NFK).

## CONFLICT OF INTEREST

The authors declare that there is no conflict of interest.

## REFERENCES

- Abraham, Y., Assefa, D. G., Hailemariam, T., Gebrie, D., Debela, D. T., Geleta, S. T., ... Manyazewal, T. (2024). Efficacy and safety of shorter multidrug-resistant or rifampicin-resistant tuberculosis regimens: a network meta-analysis. *BMC Infectious Diseases*, *24*(1), 1087. <https://doi.org/10.1186/s12879-024-09960-3>
- Beloqui, A., Solinís, M. Á., Rodríguez-Gascón, A., Almeida, A. J., & Prétat, V. (2016). Nanostructured lipid carriers: Promising drug delivery systems for future clinics. *Nanomedicine: Nanotechnology, Biology, and Medicine*, *12*(1), 143–161. <https://doi.org/10.1016/j.nano.2015.09.004>
- Bussi, C., & Gutierrez, M. G. (2019). Mycobacterium tuberculosis infection of host cells in space and time. *FEMS Microbiology Reviews*, *43*(4), 341–361. <https://doi.org/10.1093/femsre/fuz006>
- Carnero Canales, C. S., Marquez Cazorla, J. I., Marquez Cazorla, R. M., Roque-Borda, C. A., Polinário, G., Figueroa Banda, R. A., & Pavan, F. R. (2024). Breaking barriers: The potential of nanosystems in antituberculosis therapy. *Bioactive Materials*, *39*(May), 106–134. <https://doi.org/10.1016/j.bioactmat.2024.05.013>
- Chae, J., Choi, Y., Tanaka, M., & Choi, J. (2021). Inhalable nanoparticles delivery targeting alveolar macrophages for the treatment of pulmonary tuberculosis. *Journal of Bioscience and Bioengineering*, *132*(6), 543–551. <https://doi.org/10.1016/j.jbiosc.2021.08.009>
- Costabile, G., Conte, G., Brusco, S., Savadi, P., Miro, A., Quaglia, F., ... Ungaro, F. (2024). State-of-the-Art Review on Inhalable Lipid and Polymer Nanocarriers: Design and Development Perspectives. *Pharmaceutics*, *16*(3). <https://doi.org/10.3390/pharmaceutics16030347>

- De Matteis, L., Jary, D., Lucía, A., García-Embid, S., Serrano-Sevilla, I., Pérez, D., ... M. de la Fuente, J. (2018). New active formulations against M. tuberculosis: Bedaquiline encapsulation in lipid nanoparticles and chitosan nanocapsules. *Chemical Engineering Journal*, 340, 181–191. <https://doi.org/10.1016/j.cej.2017.12.110>
- Gavras, N., & Schluger, N. W. (2024). QT Prolongation Associated with Administration of Bedaquiline, a Novel Anti-Tuberculosis Drug. *Cardiology in Review*, XXX(00), 1–5. <https://doi.org/10.1097/CRD.0000000000000790>
- Gordillo-Galeano, A., Ospina-Giraldo, L. F., & Mora-Huertas, C. E. (2021). Lipid nanoparticles with improved biopharmaceutical attributes for tuberculosis treatment. *International Journal of Pharmaceutics*, 596, 120321. <https://doi.org/10.1016/j.ijpharm.2021.120321>
- Guglielmetti, L., Jaspard, M., Le Dù, D., Lachâtre, M., Marigot-Outtandy, D., Bernard, C., ... Fréchet-Jachym, M. (2017). Long-term outcome and safety of prolonged bedaquiline treatment for multidrug-resistant tuberculosis. *European Respiratory Journal*, 49(3). <https://doi.org/10.1183/13993003.01799-2016>
- Jia, B., He, J., Zhang, Y., Dang, W., Xing, B., Yang, M., ... Liu, Z. (2024). Pulmonary delivery of magnolol-loaded nanostructured lipid carriers for COPD treatment. *International Journal of Pharmaceutics*, 662, 124495. <https://doi.org/10.1016/j.ijpharm.2024.124495>
- Keck, C. M., Kovačević, A., Müller, R. H., Savić, S., Vuleta, G., & Milić, J. (2014). Formulation of solid lipid nanoparticles (SLN): The value of different alkyl polyglucoside surfactants. *International Journal of Pharmaceutics*, 474(1–2), 33–41. <https://doi.org/10.1016/j.ijpharm.2014.08.008>
- Khan, S., Sharma, A., & Jain, V. (2023). An overview of nanostructured lipid carriers and its application in drug delivery through different routes. *Advanced Pharmaceutical Bulletin*, 13(3), 446–460. <https://doi.org/10.34172/apb.2023.056>
- Khosa, A., Reddi, S., & Saha, R. N. (2018). Nanostructured lipid carriers for site-specific drug delivery. *Biomedicine and Pharmacotherapy*, 103, 598–613. <https://doi.org/10.1016/j.biopha.2018.04.055>
- Kovačević, A. B., Müller, R. H., & Keck, C. M. (2020). Formulation development of lipid nanoparticles: Improved lipid screening and development of tacrolimus-loaded nanostructured lipid carriers (NLC). *International Journal of Pharmaceutics*, 576, 118918. <https://doi.org/10.1016/j.ijpharm.2019.118918>
- Kumar, M., Virmani, T., Kumar, G., Deshmukh, R., Sharma, A., Duarte, S., ... Fonte, P. (2023). Nanocarriers in Tuberculosis Treatment: Challenges and Delivery Strategies. *Pharmaceutics*, 16(10), 1–38. <https://doi.org/10.3390/ph16101360>
- Luo, M., Zhou, W., Patel, H., Srivastava, A. P., Symersky, J., Bonar, M. M., ... Mueller, D. M. (2020). Bedaquiline inhibits the yeast and human mitochondrial ATP synthases. *Communications Biology*, 3(1), 1–10. <https://doi.org/10.1038/s42003-020-01173-z>
- Ma, J., Guan, R., Chen, X., Wang, Y., Hao, Y., Ye, X., & Liu, M. (2014). Response surface methodology for the optimization of beta-lactoglobulin nanoliposomes. *Food and Function*, 5(4), 748–754. <https://doi.org/10.1039/c3fo60476d>
- Marques, A. C., da Costa, P. C., Gonçalves, H., Catita, J., Velho, S., & Amaral, M. H. (2025). Development, optimization, and characterization of docetaxel-loaded nanostructured lipid carriers for gastric cancer treatment. *Journal of Drug Delivery Science and Technology*, 114. <https://doi.org/10.1016/j.jddst.2025.107571>
- Mauludin, R., Garmana, A. N., & Fauzian, F. (2024). Physicochemical Improvement of Carvacrol-Loaded Nanostructured Lipid Carrier (NLC). *Biointerface Research in Applied Chemistry*, 14(5). <https://doi.org/10.33263/BRIAC145.107>
- Millington, K. A., White, R. G., Lipman, M., McQuaid,

- C. F., Hauser, J., Wooding, V., ... Wingfield, T. (2024). The 2023 UN high-level meeting on tuberculosis: renewing hope, momentum, and commitment to end tuberculosis. *The Lancet Respiratory Medicine*, 12(1), 10–13. [https://doi.org/10.1016/S2213-2600\(23\)00409-5](https://doi.org/10.1016/S2213-2600(23)00409-5)
- Müller, R. H., Radtke, M., & Wissing, S. A. (2002a). Nanostructured lipid matrices for improved microencapsulation of drugs. *International Journal of Pharmaceutics*, 242(1–2), 121–128. [https://doi.org/10.1016/S0378-5173\(02\)00180-1](https://doi.org/10.1016/S0378-5173(02)00180-1)
- Müller, R. H., Radtke, M., & Wissing, S. A. (2002b). Nanostructured lipid matrices for improved microencapsulation of drugs. *International Journal of Pharmaceutics*, 242(1–2), 121–128. [https://doi.org/10.1016/S0378-5173\(02\)00180-1](https://doi.org/10.1016/S0378-5173(02)00180-1)
- Patil, S. M., Sawant, S. S., & Kunda, N. K. (2021). Inhalable bedaquiline-loaded cubosomes for the treatment of non-small cell lung cancer (NSCLC). *International Journal of Pharmaceutics*, 607, 121046. <https://doi.org/10.1016/j.ijpharm.2021.121046>
- Pornputtapitak, W., Thiangjit, Y., & Tantirungrotechai, Y. (2024). Effect of Functional Groups in Lipid Molecules on the Stability of Nanostructured Lipid Carriers: Experimental and Computational Investigations. *ACS Omega*, 9(9), 11012–11024. <https://doi.org/10.1021/acsomega.4c00685>
- Rajendhiran, N., & Bhattacharyya, S. (2024). Preparation and Evaluation of Nanolipid Carriers of Bedaquiline: In vitro Evaluation and in silico Prediction. *Jordan Journal of Pharmaceutical Sciences*, 17(3), 450–467. <https://doi.org/10.35516/jjps.v17i3.1970>
- Rajyalakshmi, K., & Boggarapu, N. R. (2019). Expected range of the output response for the optimum input parameters utilizing the modified Taguchi approach. *Multidiscipline Modeling in Materials and Structures*, 15(2), 508–522. <https://doi.org/10.1108/MMMS-05-2018-0088>
- Sabour, M. R., & Amiri, A. (2017). Comparative study of ANN and RSM for simultaneous optimization of multiple targets in Fenton treatment of landfill leachate. *Waste Management*, 65, 54–62. <https://doi.org/10.1016/j.wasman.2017.03.048>
- Sathish, T., Giri, J., Rathinasamy, S., & Kanan, M. (2024). Optimization of docetaxel-loaded cholesterol nanostructured lipid carriers for improving cancer treatment using Taguchi experimental design. *Results in Engineering*, 24, 103263. <https://doi.org/10.1016/j.rineng.2024.103263>
- Satrialdi, Putri, P. A., & Lumintang, Y. A. (2023). Pengembangan Formula Nanostructured Lipid. *Majalah Farmasi Farmakologi*, 27(2), 32–38. <https://doi.org/10.20956/mff.v27i2.27395>
- Sulek, M. W., Ogorzałek, M., Wasilewski, T., & Klimaszewska, E. (2013). Alkyl polyglucosides as components of water-based lubricants. *Journal of Surfactants and Detergents*, 16(3), 369–375. <https://doi.org/10.1007/s11743-012-1428-y>
- Viegas, C., Patrício, A. B., Prata, J. M., Nadhman, A., Chintamaneni, P. K., & Fonte, P. (2023). Solid Lipid Nanoparticles vs. Nanostructured Lipid Carriers: A Comparative Review. *Pharmaceutics*, 15(6). <https://doi.org/10.3390/pharmaceutics15061593>
- Wei, S., He, C., Xie, X., Zhang, A., Tang, S., Li, S., & He, Y. (2024). Which fluoroquinolone is safer when combined with bedaquiline for tuberculosis treatment: evidence from the FDA Adverse Event Reporting System database from 2013 to 2024. *Frontiers in Pharmacology*, 15. <https://doi.org/10.3389/fphar.2024.1491921>
- Yadav, S., Rawal, G., & Baxi, M. (2016). Bedaquiline: A novel antitubercular agent for the treatment of multidrug-resistant tuberculosis. *Journal of Clinical and Diagnostic Research*, 10(8), FM01–FM02. <https://doi.org/10.7860/JCDR/2016/19052.8286>